

# Uptake of NO<sub>3</sub> on liquid surfaces

Matthias Schütze and Hartmut Herrmann

## Introduction

NO<sub>3</sub> which is formed in the reaction of NO<sub>2</sub> with ozone can reach concentration levels up to 10<sup>9</sup> molecules per cm<sup>3</sup> in the night time atmosphere. Its gas phase reactions with many compounds, e.g. olefins, are fast and may represent import loss pathways at night. In wet atmospheric particles such as cloud drops, NO<sub>3</sub> can initiate radical reactions leading to the oxidation of S(IV) compounds and to halogen activation from Cl<sup>-</sup> and Br<sup>-</sup> (Finlayson-Pitts & Pitts, 2000). The phase transfer of the radical across atmospheric liquid surfaces such as cloud droplets can act as an import loss or sink process for either phase.



Fig. 1: Single drop hanging on a pipette's tip inside a flow tube gas phase reactor

## Single drop experiment

A single drop experiment (Schütze & Herrmann, 2002) was used for the investigation of the transfer from the gas phase into an aqueous drop. It consists of a flow-tube reactor including a section for generation and analysis of single liquid drops. The drops are suspended on the tip of a pipette, see Figure 1. The light of a broad banded source is fed through an optical fibre inside the pipette to its tip. After passing the drop as an absorption path way the light is coupled into a second fibre which leads to a diode array spectrometer for detection. This set-up allows *in situ* monitoring of the liquid phase concentrations.

## Set-up I

The basic flow tube shown in Fig. 2 is 30 cm long and 2.13 cm in diameter. It was fed with humidified Helium as a carrier gas through the main inlet. N<sub>2</sub>O<sub>5</sub> was introduced via the lateral precursor inlet and thermalized by an electrical heater right before entering the main tube. This produced NO<sub>3</sub> (beside NO<sub>2</sub>). The concentration of NO<sub>3</sub> is determined after reaction with an organic which is introduced at the position of the drop through the movable inlet. The concentration of the organic is monitored by GC-FID. The drops were made of aqueous solutions of the dye Alizarin Red S (ARS) which acted as a scavenger for the NO<sub>3</sub> that entered the liquid phase. The strong absorbance of the dye was followed for quantification of the uptake.

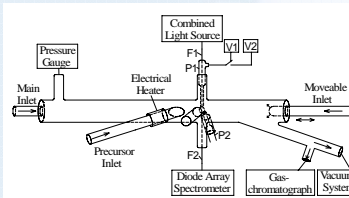


Fig. 2: Schematic diagram of the basic flow tube reactor

## Set-up II

The basic flow tube was extended by a heated pre-reactor upstream the main tube and by a UV-VIS absorption cell downstream. NO<sub>3</sub> was produced from the reaction of NO<sub>2</sub> and O<sub>3</sub> at 393 K in the pre-reactor (1 m long, 3.5 cm i.d.). It was detected by its absorption at 662 nm. For the determination of the other N-containing species present, the UV-VIS cell was replaced by a FT-IR spectrometer equipped with a white cell. The drops consisted of aqueous NaCl solutions. The uptake of the NO<sub>3</sub> radical was monitored by the absorption of the nitrate ions formed in the drop after reaction of NO<sub>3</sub> with Cl<sup>-</sup> or other constituents of the solution.

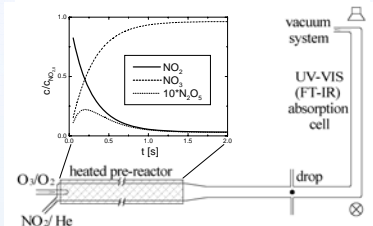


Fig. 3: Schematic diagram of the extended flow tube reactor including heated pre-reactor and UV-VIS (FT-IR) absorption cell. The result of a model simulation of the reaction system is shown in the inset

## Uptake on ARS solutions

A drop of ARS solution exposed to a NO<sub>3</sub> containing gas flow shows a time dependent absorbance as shown in Fig. 3.

Around 430 nm the absorbance is decreasing indicating the degradation of the dye. At wavelengths below 400 nm the absorbance is increasing which is attributed to the formation of products from the reaction of NO<sub>3</sub> with the dye. The uptake of NO<sub>3</sub> was monitored by following the decaying absorbance of ARS.

The measured time course of the absorbance at 450 nm (corrected by the absorbance at 600 nm) depending on the initial ARS concentration is presented in Fig. 4. For the lowest dye concentrations, a decreasing slope indicates some kind of saturation effect. Nevertheless, this is not the case for the highest concentrations used.

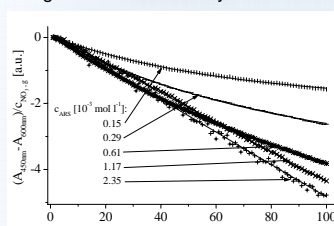


Fig. 4: Plot of the ARS absorbances at 450 nm for the different dye concentrations used. For comparison, all plots are normalized with the measured gas phase NO<sub>3</sub> concentration.

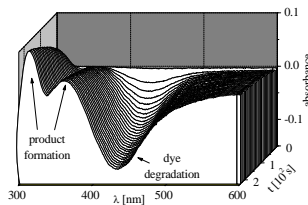


Fig. 3: Time dependent absorbance of a drop of ARS solution exposed to gas phase NO<sub>3</sub>

An uptake coefficient of  $\gamma_{\text{NO}_3} = (2.7 \pm 0.8) \cdot 10^{-3}$  was calculated from the initial slopes of these plots. After correction for the effect of the limited gas phase diffusion, a lower limit for the mass accommodation coefficient is obtained:

$$\alpha_{\text{NO}_3} \geq 2.4 \cdot 10^{-3}$$

## Gas phase composition

NO<sub>2</sub> reacted with an excess of ozone to form NO<sub>3</sub>. Nevertheless, no NO<sub>3</sub> was found in the UV-VIS cell if the heater of the pre-reactor was switched off (Case A in Fig. 5). This is due to the reaction of NO<sub>2</sub> with NO<sub>3</sub> which forms N<sub>2</sub>O<sub>5</sub>. A mixture of N<sub>2</sub>O<sub>5</sub> and HNO<sub>3</sub> was found using FT-IR. The occurrence of nitric acid is attributed to the conversion of N<sub>2</sub>O<sub>5</sub> on the reactor walls which carry small amounts of water even under very low relative humidities (RH).

When the heater is switched on (Case B) the N<sub>2</sub>O<sub>5</sub> decomposes very rapidly. Consequently, the measured NO<sub>3</sub> concentration accounts for more than 90 % of the initial NO<sub>2</sub>.

Upon increasing the relative humidity to 90 %, the NO<sub>3</sub> concentration dropped to less than 60 % of the initial NO<sub>2</sub> concentration (Case D). NO<sub>3</sub> seems to be converted efficiently on the humid reactor walls. Surprisingly, the lost NO<sub>3</sub> was recovered as HNO<sub>3</sub> in the gas phase!

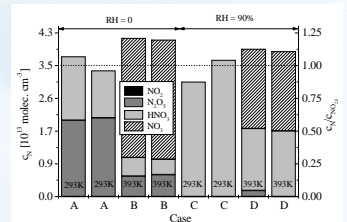


Fig. 5: Gas phase composition measured by UV-VIS and FT-IR spectroscopy.

Case A: RH = 0; T<sub>heater</sub> = 293 K  
Case B: RH = 0; T<sub>heater</sub> = 393 K  
Case B: RH = 90%; T<sub>heater</sub> = 293 K  
Case B: RH = 90%; T<sub>heater</sub> = 393 K

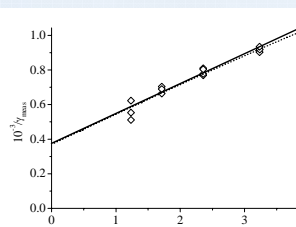


Fig. 6: Uptake of NO<sub>3</sub> on NaCl solutions, plot of 1/γ<sub>meas</sub> versus a<sub>Cl<sup>-</sup></sub><sup>-0.5</sup>.

## Uptake on NaCl solutions

After uptake on solutions of NaCl, the NO<sub>3</sub> radical reacts with chloride to form the NO<sub>3</sub><sup>-</sup> ion.

This was used to quantify the uptake of NO<sub>3</sub>. Fig. 6 shows the resulting uptake coefficients γ<sub>meas</sub> depending on the chloride activity a<sub>Cl<sup>-</sup></sub>. Extrapolating γ<sub>meas</sub> to 1/a<sub>Cl<sup>-</sup></sub><sup>-0.5</sup> = 0 (corresponding to an infinitely fast liquid phase reaction) and correcting for the limiting effect of gas phase diffusion yields a value for α<sub>NO<sub>3</sub></sub>:

$$\alpha_{\text{NO}_3} = (4.2^{+2.2}_{-1.7}) \cdot 10^{-3}$$

This is consistent with the ARS measurements.

## Literature

- Finlayson-Pitts, B.J., Pitts, J.N.Jr. (2000). *Chemistry of the Upper and Lower Atmosphere*. New York, Academic Press  
Schütze, M., & Herrmann, H. (2002). Determination of phase transfer parameters for the uptake of HNO<sub>3</sub>, N<sub>2</sub>O<sub>5</sub> and O<sub>3</sub> on single aqueous drops, *Phys. Chem. Chem Phys.*, 4, 60-67.